Seasonal stress modulation on active California fault structures

Report for SCEC Award #16006
Submitted July 4, 2017

Investigators: Roland Bürgmann (UCB), Christopher Johnson (UCB), Pierre Dutilleul (McGill)

I. Project Overview

A. Abstract

In the box below, describe the project objectives, methodology, and results obtained and their significance. If this work is a continuation of a multi-year SCEC-funded project, please include major research findings for all previous years in the abstract. (Maximum 250 words.)

In California, the accumulation of winter snowpack in the Sierra Nevada, water in lakes and reservoirs, and groundwater in basins follow the annual cycle of wet winters and dry summers. These seasonal changes in water storage produce elastic deformation of the Earth's crust and micro-earthquakes appear to follow a subtle annual cycle, possibly in response to the water load. Previous studies posit that temperature, atmospheric pressure, or hydrologic changes may promote additional earthquakes above background levels. Here we use GPS vertical time series (2006 – 2015) to constrain models of monthly hydrospheric loading and compute stresses on faults throughout California, which can exceed 1kPa. Depending on fault geometry the addition or removal of water increases the Coulomb failure stress. The largest stress amplitudes are occurring on dipping reverse faults in the Coast Ranges and along the eastern Sierra Nevada range front. We analyze M≥2.0 earthquakes with known focal mechanisms in northern and central California to resolve fault normal and shear stresses for the focal geometry. Our results reveal more earthquakes occurring during slip-encouraging stress conditions and suggest that earthquake populations are modulated at periods of natural loading cycles, which promote failure by subtle stress changes. The most notable shear-stress change occurs on more shallowly dipping structures. However, vertically dipping strike-slip faults are common throughout California and experience smaller amplitude stress change but still exhibit positive correlation with seasonal loading cycles. Our analysis suggests the annual hydrologic cycle is a viable mechanism to promote earthquakes and provides new insight to fault mechanical properties.

B. SCEC Annual Science Highlights

Each year, the Science Planning Committee reviews and summarizes SCEC research accomplishments, and presents the results to the SCEC community and funding agencies. Rank (in order of preference) the sections in which you would like your project results to appear. Choose up to 3 working groups from below and re-order them according to your preference ranking.

Seismology

Tectonic Geodesy

Stress and Deformation Through Time (SDOT)

C. Exemplary Figure

Select one figure from your project report that best exemplifies the significance of the results. The figure may be used in the SCEC Annual Science Highlights and chosen for the cover of the Annual Meeting Proceedings Volume. In the box below, enter the figure number from the project report, figure caption and figure credits.

Figure 2 (A) Seasonal Coulomb stress resolved on the SCEC Community Fault Model. This one-month snapshot indicates a peak stress change of 1.5 kPa during the fall months in 2009. **(B)** Representative time series of seasonally modulated Coulomb stress on the central SAF indicate a peak-to-peak stress cycle of ~700 Pa. **(C)** Faulting mechanism resolved from 1984-2014 M≥2.0 focal mechanisms for area outlined in the map. Distributions indicate strike-slip and reverse events occur more often in the spring and fall months.

D. SCEC Science Priorities

In the box below, please list (in rank order) the SCEC priorities this project has achieved. See *https://www.scec.org/research/priorities* for list of SCEC research priorities. *For example: 6a, 6b, 6c*

We directly address the SCEC4 Research Priorities and Requirements by exploring the response of seismicity to a well-characterized periodic forcing function. While hydrological loads are not explicitly mentioned, this work addresses several of the problems in earthquake physics called out by SCEC4 including stress transfer, stress-mediated fault interactions and earthquake clustering, and causes and effects of transient deformations. This work address science objectives 2b, 2d, 2f. This work utilized the SCEC Community Fault Model.

E. Intellectual Merit

How does the project contribute to the overall intellectual merit of SCEC? *For example: How does the research contribute to advancing knowledge and understanding in the field and, more specifically, SCEC research objectives? To what extent has the activity developed creative and original concepts?*

We directly address the SCEC4 Research Priorities and Requirements by exploring the response of seismicity to a well-characterized periodic forcing function. While hydrological loads are not explicitly mentioned, this work addresses several of the problems in earthquake physics called out by SCEC4 including stress transfer, stress-mediated fault interactions and earthquake clustering, and causes and effects of transient deformations. We rely on the CFM product, our own stress inversions, and catalogs of focal mechanisms to refine our analysis by considering where the transient stress cycles act in parallel with the background stress.

F. Broader Impacts

How does the project contribute to the broader impacts of SCEC as a whole? *For example: How well has the activity promoted or supported teaching, training, and learning at your institution or across SCEC? If your project included a SCEC intern, what was his/her contribution? How has your project broadened the participation of underrepresented groups? To what extent has the project enhanced the infrastructure for research and education (e.g., facilities, instrumentation, networks, and partnerships)? What are some possible benefits of the activity to society?*

The seismic hazards of active plate boundary faults will affect more individuals as the population of California continues to increase. This project improves our ability to characterize the time-dependent stresses on active faults in California by investigating the seismicity response to seasonal loading along the plate boundary. An improved understanding of earthquake physics to better characterize the effect of transient loading will lead to improved forecast models in future endeavors.

The project has supported a graduate student and fostered collaborations for that student with more senior members of the SCEC scientific community. The collaborations developed by young scientist is integral to the advancement of new ideas and research directions. The student supported by this project is also actively participating in the SCEC Community Geodetic Model initiative.

Portions of this work are now included in classroom lectures and lab components on topics of active tectonics and structural geology to further the understanding of fault mechanics and fault interaction. Additionally the material is presented to middle school aged students through a graduate student outreach program led by the SCEC supported graduate student. These outreach activities are designed to raise public awareness at a young age and provide a basic understanding of the geologic environment in which they live and what to do in the event of an earthquake.

G. Project Publications

Dutilleul, P., C. W. Johnson, R. Bürgmann, Y. Wan, and Z.-K. Shen (2015), Multifrequential periodogram analysis of earthquake occurrence: An alternative approach to the Schuster spectrum, with two examples in central California, Journal of Geophysical Research: Solid Earth, 120(12), 8494-8515. SCEC contribution number 6160

Johnson, C.W., R. Bürgmann, Y. Fu, and Dutilleul, P (2015) Seasonal water storage, the resulting deformation and stress, and occurrence of earthquakes in California, SCEC Annual Meeting 2015.

Johnson, C.W., R. Bürgmann, Y. Fu, and Dutilleul, P (2015) Seasonal water storage, the resulting deformation and stress, and occurrence of earthquakes in California, AGU Fall Meeting 2015, G54A-05.

Johnson, C.W., Y. Fu , and R. Bürgmann, 2016, Seasonal stress modulation on active California fault structures, AGU 2016 Fall Oral Presentation. G41A-03. San Francisco, CA.

Johnson, C.W., R. Bürgmann, Y. Fu, and P. Dutilleul, 2016, Seasonal stress modulation on active California fault structures, Stress State of the Earth, Los Alamos, NM, invited talk.

Johnson, C.W., R. Bürgmann, Y. Fu, and P. Dutilleul, 2016, Seasonal stress modulation on active California fault structures, Southern California Earthquake Center Annual Meeting 2016, Palm Springs, CA.

Johnson, C.W., R. Bürgmann, Y. Fu, and P. Dutilleul, 2016, Seasonal Water Storage, the Resulting Deformation and Stress, and Occurrence of Earthquakes in California, UNAVCO Workshop 2016, Hydrology Section. Boulder, CO.

Johnson, C. W., Y. N. Fu, and R. Bürgmann (2017), Seasonal water storage, stress modulation, and California seismicity, Science, 356(6343), 1161-1164, doi:10.1126/science.aak9547.

Johnson, C.W., Y. Fu , and R. Bürgmann, 2017, Seasonal stress modulation on active California fault structures, 2017 Computation in Geophysics Workshop. Denver, CO, invited.

Johnson, C.W., Y. Fu , and R. Bürgmann, 2017, Seasonal stress modulation on active California fault structures, EarthScope National Meeting. Anchorage, AK.

All publications and presentations of the work funded must be entered in the SCEC Publications database. Log in at *http://www.scec.org/user/login* and select the Publications button to enter the SCEC Pubications System. Please either (a) update a publication record you previously submitted or (b) add new publication record(s) as needed. If you have any problems, please email *web@scec.org* for assistance.

II. Technical Report

A. Significance and Objectives

Data from the PBO continuous GPS network allowed Argus et al. [2014], Amos et al. [2014] and Borsa et al. [2014] to document crustal deformation in California associated with seasonal changes in hydrospheric surface loads (groundwater, surface water, snow), as well as regional uplift due to the on-going drought in the western U.S., notably in California. This dense network of continuous GPS stations allows real-time monitoring of crustal water storage (Figure 1). Annual vertical and horizontal displacement amplitudes of GPS stations in the Sierra Nevada and California Coast Ranges produced by seasonal changes in water storage are on the order of 1-5 mm and 0.5-2 mm, respectively [*Amos et al.*, 2014]. Water loss due to drought conditions in recent years resulted in longer-term uplift of areas surrounding the Central Valley at rates of up to ~5 mm/yr [*Amos et al.*, 2014; *Borsa et al.*, 2014]. In contrast, stations in the Central Valley and other young sedimentary basins rise and fall with the groundwater level in the aquifer below due to the poroelastic response to changes in water head [*Chaussard et al.*, 2014].

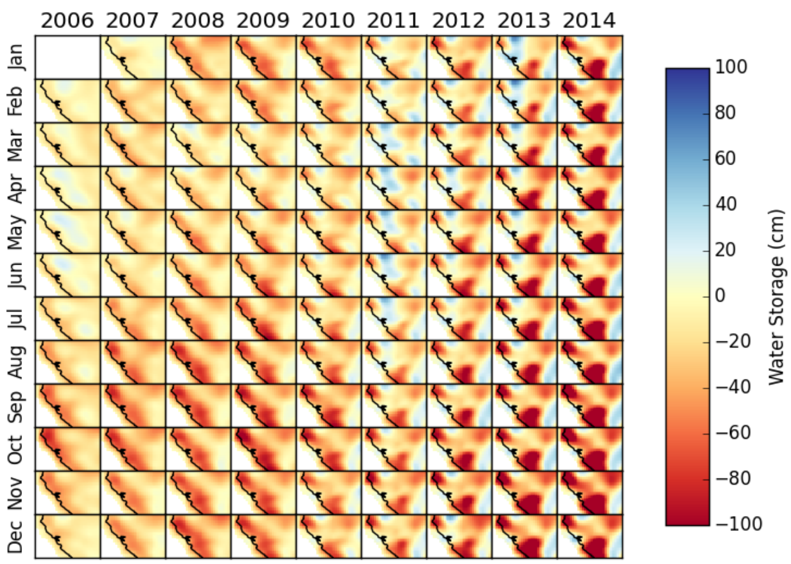

Figure 1. Distributed surface load shown as a monthly time series in seasonal water storage (equivalent water thickness) derived from GPS vertical displacements between 2006-2014. The load is distributed on a 0.25˚ x 0.25˚ grid throughout California and Nevada. We use this surface load to produce 3D models of time-dependent deformation and stress using a spherical, layered Earth model [*Pollitz et al.*, 2013]. Variations in the amplitude, phase and orientation of the load-induced stress field is compared with variations in the rate, location and focal mechanisms of small earthquakes.

Knowledge of what governs the timing of earthquakes is essential to understanding the nature of the earthquake cycle and to determining time-dependent earthquake hazard, yet the variability and controls of earthquake occurrences are not well established. If slight changes in static stress influence the timing of earthquakes, either promoting or discouraging nucleation, then one could expect that earthquakes will occur more often during periods of preferential surface loading conditions. Seasonal crustal stress variations can result from hydrospheric and atmospheric surface loads [*Amos et al.*, 2014; *Dong et al.*, 2002; *Gao et al.*, 2000; *Heki*, 2003; *Holzer*, 1979; *Namias*, 1989], fluctuations of subsurface pore fluid pressures [*Christiansen et al.*, 2007; *Hainzl et al.*, 2013], and thermoelastic strains from atmospheric temperature variations [*Ben-Zion and Allam*, 2013]. A number of studies suggest that seismicity correlates with seasonal forcing [*Bettinelli et al.*, 2008; *Christiansen et al.*, 2007; *Gao et al.*, 2000; *Hainzl et al.*, 2013; *Heki*, 2003; *Pollitz et al.*, 2013]. In California, seasonal cycles of snow and water loads in the Sierra Nevada and Central Valley [*Amos et al.*, 2014; *Argus et al.*, 2014] may help drive such periodic seismicity patterns [*Christiansen et al.*, 2007; *Gao et al.*, 2000; *Zaliapin and Ben-Zion*, 2013]. The lack of observational documentation of the statistical significance of such modulation in natural earthquake populations has so far limited the consideration of small stress changes in time-dependent earthquake forecasting.

Simple models of stress changes on the San Andreas (SAF) and other nearby faults from the associated elastic deformation suggest seasonal stress cycles of up to ~1 kPa [*Amos et al.*, 2014], comparable to those associated with the short-period solid Earth tides [*Thomas et al.*, 2012]. While modest compared to annual interseismic fault loading rates of 5-50 kPa/yr [*Parsons*, 2006; *Smith and Sandwell*, 2006], the long period of the stress cycles (comparable to duration of earthquake nucleation) may be expected to allow for detectable modulation of crustal seismicity from these seasonal load cycles [*Beeler and Lockner*, 2003].

Detailed investigations of focal mechanisms in southern California reveal a heterogeneous stress field and variations in faulting style [*Yang and Hauksson*, 2013] that need to be considered when investigating the effect of applied stress transients on fault activity. In this study we rigorously characterize the seasonal periodicity in the seismicity catalog, model seasonal deformation and stress, and evaluate changes in location and mechanisms of earthquakes to better understand the effects of small stress changes resulting from varying surface loads in California.

The project results spatially and temporally characterize the near surface water storage and test the sensitivity of earthquake occurrence with respect to small external stressing due to seasonal changes in hydrospheric surface loads. Completed thus far is the analysis of statistical significance of observed periodicities in California seismicity records [*Dutilleul et al.*, 2015] and hydrospheric load modeling to describe the temporally changing stresses on active fault structures that modulate low magnitude seismicity [*Johnson et al.*, 2017]. The published and preliminary results for additional components of the study have been presented at conferenced listed 1G. Continued modeling efforts are underway to describe addition loading cycles and the possible stressing contribution to the hydrological loading cycle and further describe the modulation of seismicity on California faults.

B. Statistical Significance of Detected Periodicity in CA Earthquake Occurrence

Periodicities in earthquake occurrence may represent seasonally varying conditions due to changes in hydrospheric loads. We explore seismicity catalogs in two regions of CA, one near the central SAF and the second in the Sierra Nevada – Eastern California Shear Zone (SN-ECSZ), for periodic behavior using three independent statistical tests. To ensure a robust analysis, we test 26 years of M≥2.5 catalog data and apply two declustering methods. The first is the [*Reasenberg*, 1985] method developed for northern and central California. The second is a spatial-temporal ETAS model that estimates the probability that an event is a background earthquake [*Zhuang et al.*, 2002]. Both methods are widely used and appropriate for the purpose of testing the regions of interest. We consider both the original earthquake catalogs as well as subsets made of declustered events that separate dependent seismic activity produced by fault interaction, including foreshocks and aftershocks, from independent background earthquakes, including mainshocks and single events [*van Stiphout et al.*, 2012], thereby testing a total of six catalogs. We examine to what degree the choice of declustering algorithm [*Reasenberg*, 1985; *Zhuang et al.*, 2002] affects the results of our analysis. The statistical analyses are described in last year's technical report and full details are published in [*Dutilleul et al.*, 2015].

Near Parkfield, CA we find strong evidence for annual periods in earthquake occurrence, consistent with previous results suggesting seasonal modulation of seismicity [*Christiansen et al.*, 2007]. The results indicate statistically significant periods of about 4-, 6-, and 12-months for seismicity located on the SAF near Parkfield. For this region we find peak earthquake occurrence in the dry fall months of August and September and a secondary peak in activity in April. Similarly, in the SN-ECSZ we find a statistically significant annual period, as well as a ~14 month period that we specifically test for in order to consider the period of pole-tide induced stresses. The results indicate the declustering methods reduce the periodic component resolved in the time series, but do not produce a Poissonian process since we are able to resolve similar periods when compared to the original time series.

We find that there is significant annual periodicity in earthquakes along the central SAF and adjacent Coast Ranges that appears to reflect seasonal loading from hydrospheric and tidal loads. We explore the phase and amplitude information of periodic sources of stress including the pole tides, annual and semi-annual tides, and annual hydrological load cycles. The pole tides and the semi-annual and annual tides are estimated following *Shen et al.* [2005] and *Agnew* [1997], respectively, and both oscillate at the same phase for periods of interest in California, with the amplitude determined by the latitude. Modeled peak-to-trough shear-stress amplitudes on the CSAF from the pole-tides and tides are of order 100 Pa and combine to produce sub-equal peaks of stress encouraging right-lateral slip in the spring and fall. Fault-normal pole-tide stress on the CSAF has an amplitude of > 700 Pa, with annual components of ~200 Pa and peak tension in the spring. Fault-normal peak-to-trough stress amplitude from the tides is only 30 Pa. Normal-stress cycles from seasonal hydrological unloading have been estimated to be of order ~1000 Pa peak-to-trough, with greatest tensile stress in October during the drier months. This suggests that the fall peak in earthquake occurrence is due to the dominantly fault-normal stress cycles of hydrological surface loads, while the second peak in the spring may be related to stress cycles from the pole-tide and tidal contributions, which indicate a peak shear stress in March and September. The occurrence of two peaks in seismicity at times when the normal stress is favorable for fault unloading conditions would suggest the fault is encouraged to slip by shear stress change of order 100 Pa, considerably less than static or dynamic stress changes typically associated with earthquake triggering. The modulation of seismicity with a period of one-year supports our hypothesis of seasonal loading and warrants our continued efforts to model the seasonal deformation associated with these time varying loads.

C. Time Varying Stresses on the Community Fault Model and Focal Mechanism Catalog

Modeling the time-dependent surface loading allows us to calculate the expected deformation from the addition or removal of mass from the Earth's surface using the near-surface water storage derived from vertical GPS displacements (Figure 1). The equivalent water storage is inverted from cGPS and represents the volume mass change in the hydrosphere that extends from 32˚N – 42.5˚N and 125˚W – 115˚W on a 0.25˚x0.25˚ grid and is resolved for a monthly time-series between 2006-2014. This water storage is used as a model input to calculate the deformation at both the surface and seismogenic depths (8 km). We implement an elastic mechanical model on a spherically stratified Earth model based on the preliminary reference Earth model (PREM) and generate a time-series of the deformation that corresponds to the spatially varying distributed water storage in the near surface. The static displacements are calculated using a modified version of STATIC1D [*Pollitz*, 1996; 1997] that is adapted for a vertical force at the surface and calculates the equations of static equilibrium. The calculated surface displacements are used to validate the model by comparing to the GPS time series. The deformation at 8 km depth is used to estimate the load-induced stresses.

The induced stress changes from hydrospheric loading are computed for both the fault geometry in the SCEC Community Fault Model [Field et al., 2013] and with focal mechanisms in the study region to resolve site-specific time-varying stresses throughout California. The fault model provides the location and the average strike, dip, and rake for CA faults. This allows high spatial and temporal sampling of transient deformation on these active structures. Figure 2 shows the average peak-to-peak shear, normal, and Coulomb (μ=0.1 and 0.7) stress change during the 9-year study period. The shallowly dipping structures adjacent to the central valley experience and the eastern Sierra Nevada bounding faults show the largest transient stress change. The time-series shown in Figure 2 is an example from the central SAF, dipping 90˚, and experiencing a stress change from the surface load with a peak-to-peak amplitude of 0.7 kPa. Our initial analysis of the seismicity in the immediate vicinity of the coast range reverse faults outlined in Figure 2 suggest the occurrence of more events during the months of loading conditions in excess of 500 Pa that encourage failure. Similarly, we find more events occurring on strike-slip faults during favorable loading conditions, but lower in amplitude when compared to the revers faults.

Additionally, we look at the focal plane orientation of events and explore the stresses resolved for the fault plane orientation (Figure 3). The focal mechanism results are produced using the first motion phase arrivals available through the Northern California Earthquake Data Center (http://ncedc.org) with the FPFIT algorithm [Reasenberg and Oppenheimer, 1985] for M≥2 events between 2006 through 2014 for northern and central California. The algorithm uses a grid search method to minimize the misfit of the P-wave first-motion polarities using the available phase information. To ensure high-quality focal mechanisms we require a minimum of 25 observations to calculate a solution and eliminate many solutions that are below our standards. We remove all focal mechanism solutions that do not converge, have a station distribution ratio <0.55, or if the strike, dip, and rake error is >35˚. The station distribution ratio is the best quantitative measure of the quality of the FPFIT solution [*Kilb and Hardebeck*, 2006].

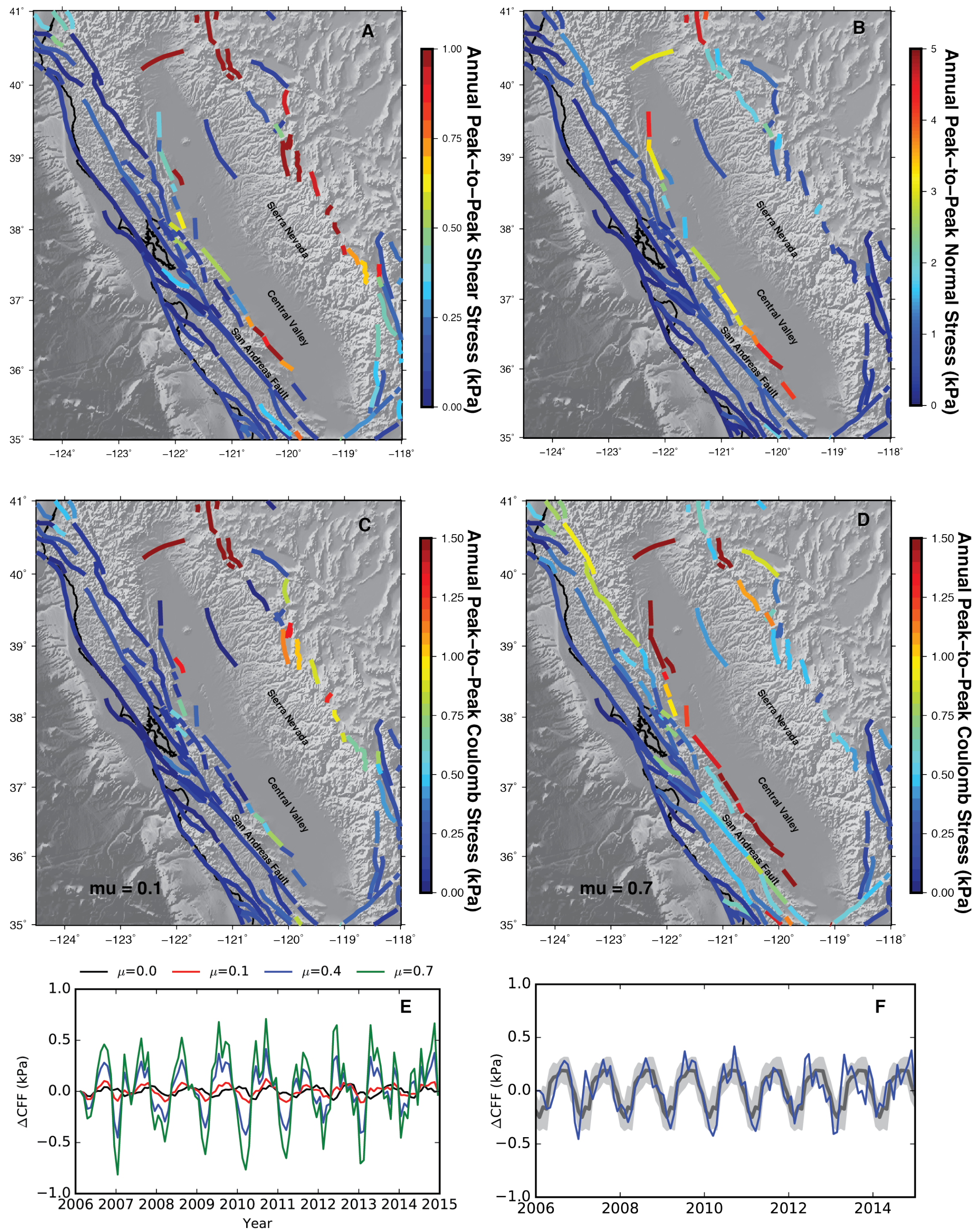

Figure 2. Seasonal average peak-to-peak (A) shear and (B) normal stress changes resolved on the UCERF3 California statewide fault model. (C) The Coulomb stress using a friction coefficient of 0.1. (D) The Coulomb stress using a friction coefficient of 0.7. (E) The times series of Coulomb stress changes on the central San Andreas fault for friction coefficients of 0.0, 0.1, 0.4, 0.7. (F) The central San Andreas Fault estimated annual stress (dark gray line) with one standard deviation (grad shading) for the hydrological induced Coulomb (μ=0.4) stress change (blue line).

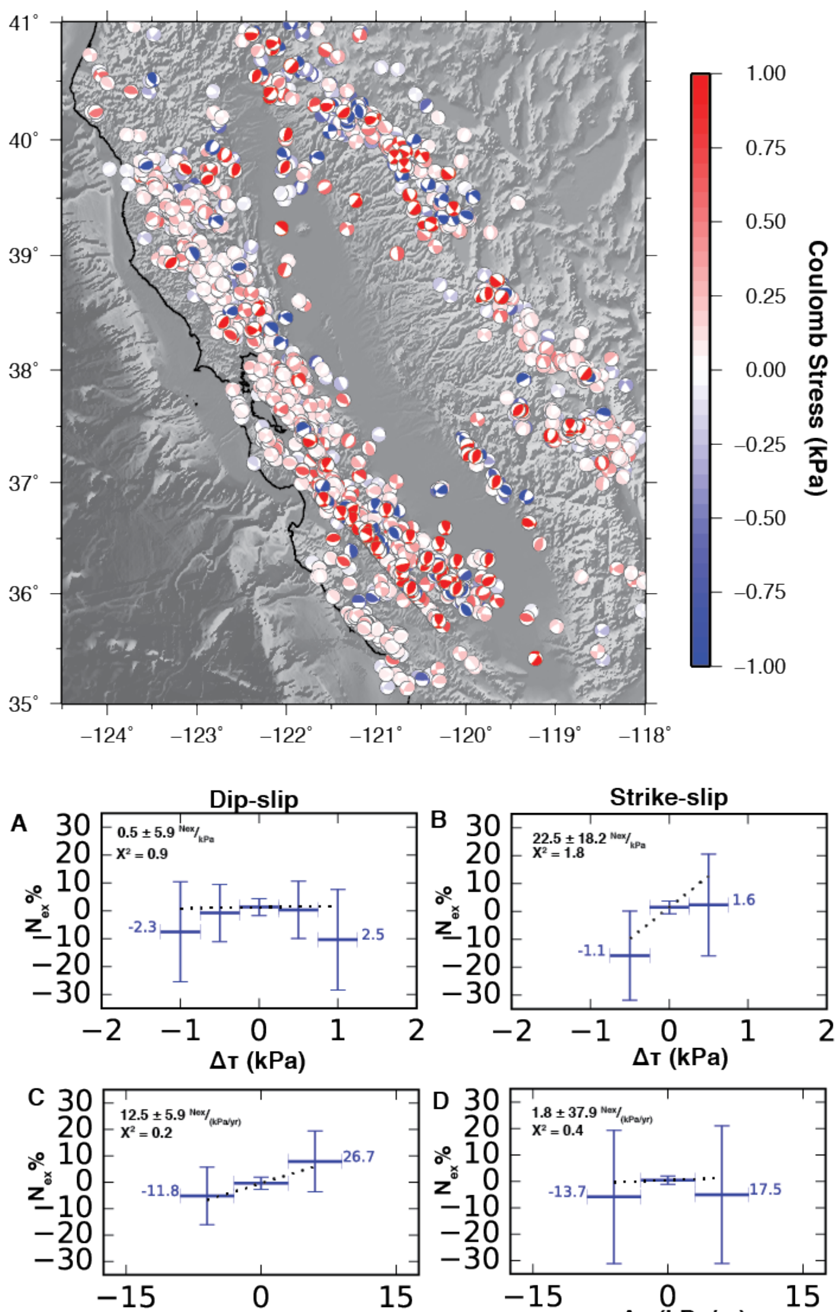

Figure 3. (Top)The hydrological surface loading Coulomb stress change is indicated by the color of the shaded focal mechanism compression quadrant for M≥2.0 events from 2006-2015. Events with a ±0.05 stress change are not shown. (Bottom) Excess seismicity plots for dip-slip and strike-slip events showing results for both peak stress amplitude and peak stress rate.

In Figure 3 we quantify the percent excess seismicity (N_{Ex}) using 0.5 kPa and 6.0 kPa/yr stress intervals centered on zero for the resolved stress amplitude and stressing rate, respectively. The focal mechanisms shown in the top panel are separated into populations of dip-slip containing the reverse, normal, and oblique events (N=2,345) and strike-slip (N=1,344) events. The bottom panels show the results for the shear stress amplitude and rate for the dip-slip and strike-slip events. A positive trend is observed for the shear stress amplitude and the strike-slip events of 22.5 ± 18.2 N_{ex}/kPa (at 95% confidence) between -1.1 and 1.6 kPa, indicating a seismic response to the peak shear amplitude. The dip-slip events exhibit a response to the shear stressing rate with a positive trend of 12.5 ± 5.9 N_{ex}/kPa/yr, ranging from -11.8 to 26.7 kPa/yr. Excess events are not observed for the strike-slip events from an increase in the shear stressing rate and similarly the dip-slip events do not show excess seismicity as the shear stress amplitude increases. The N_{Ex} values indicate that earthquakes are occurring at different times of the shear stress cycle for different fault types, suggesting that the strike-slip events are mechanically different from the dip-slip population. Full details of the analysis are published [*Johnson et al.*, 2017].

D. Findings and Ongoing Analysis

The 3-year project consists of four primary components: (i) evaluate the statistical significance of detected periods in seismicity catalogs for events located along the SAF and in the SN-ECSZ, (ii) develop elastic deformation models of monthly surface loads, (iii) evaluate the degree of correlation between model stress cycles and seismicity taking into consideration the variable amplitude of stress cycles, the orientation of transient load stress with respect to the background stress field, and the geometry of active faults revealed by focal mechanisms, and (iv) analyze loading cycles of additional natural cycles that produce stress changes on fault systems. The first component is complete and indicates significant annual periods in the seismicity records. The second and third component are complete when considering hydrological loading cycles. We find seismicity occurring more often during periods of favorable stress conditions of focal plane orientations for M≥2.0 earthquakes. For the fourth component we will carefully explore to what degree other sources of periodic stress at annual or similar periods will need to be considered. To complete the fourth component models will be produced to obtain an aggregate seasonal stress change from hydrological, atmosphere, temperature, ocean tide, pole-tide, and body-tide. The combined total periodic stresses will be evaluated to examine the largest source of loading on each fault system contained in the CFM. The seismicity will be examined with respect to the regional stress orientation. A background stress field will be inverted from 35 years of focal mechanism data [*Hardebeck and Michael*, 2006]. We will test for systematic changes in the background stress during loading cycles and look for excess seismicity above background levels as seasonal stresses increase in the principal component orientation. This analysis will provide additional information to the stress changes that are modulating seismicity.

E. References

Agnew, D. C. (1997), NLOADF: A program for computing ocean-tide loading, *Journal of Geophysical Research*, *102*(B3), 5109-5110, doi:10.1029/96jb03458.

Amos, C. B., P. Audet, W. C. Hammond, R. Bürgmann, I. A. Johanson, and G. Blewitt (2014), Contemporary uplift and seismicity in central California driven by groundwater depletion, *Nature*, *509*, 483-486, doi:10.1038/nature13275.

Argus, D. F., Y. Fu, and F. Landerer (2014), GPS as a high resolution technique for evaluating water resources in California, *Geophys. Res. Lett.*, *41*, doi: 10.1002/2014GL059570.

Beeler, N. M., and D. A. Lockner (2003), Why earthquakes correlate weakly with the solid Earth tides: Effects of periodic stress on the rate and probability of earthquake occurrence, *J. Geophys. Res.*, *108*(B8), doi:10.1029/2001jb001518.

Ben-Zion, Y., and A. A. Allam (2013), Seasonal thermoelastic strain and postseismic effects in Parkfield borehole dilatometers, *Earth Planet. Sci. Lett.*, *379*, doi:10.1016/j.epsl.2013.1008.1024.

Bettinelli, P., J.-P. Avouac, M. Flouzat, L. Bollinger, G. Ramillien, S. Rajaure, and S. Sapkota (2008), Seasonal variations of seismicity and geodetic strain in the Himalaya induced by surface hydrology, *Earth Planet. Sci. Lett.*, *266*, 332-344, doi:10.1016/j.epsl.2007.11.021.

Borsa, A. A., D. C. Agnew, and D. R. Cayan (2014), Ongoing drought-induced uplift in the western United States, *Science*, *345*(6204), 1587-1590.

Chaussard, E., R. Bürgmann, M. Shirzaei, E. Fielding, and B. Baker (2014), Predictability of hydraulic head changes and characterization of aquifer system and fault properties from InSAR-derived ground deformation, *J. Geophys. Res.*, *119*(8), 6572-6590, doi:10.1002/2014JB011266.

Christiansen, L. B., S. Hurwitz, and S. E. Ingebritsen (2007), Annual modulation of seismicity along the San Andreas Fault near Parkfield, CA, *Geophys. Res. Lett.*, *34*(L04306), doi:10.1029/2006GL028634.

Dong, D., P. Fang, Y. Bock, M. K. Cheng, and S. Miyazaki (2002), Anatomy of apparent seasonal variations from GPS-derived site position time series, *J. Geophys. Res.*, *107*(B4), doi:10.1029/2001JB000573.

Dutilleul, P., C. W. Johnson, R. Bürgmann, Y. Wan, and Z.-K. Shen (2015), Multifrequential periodogram analysis of earthquake occurrence: An alternative approach to the Schuster spectrum, with two examples in central California, *Journal of Geophysical Research: Solid Earth*, *120*(12), 8494-8515, doi:10.1002/2015JB012467.

Field, E. H., et al. (2013), Uniform California earthquake rupture forecast, version 3 (UCERF3) The time-independent model: U.S. Geological Survey Open-File Report 2013-1165, *California Geological Survey Special Report 228, and Southern California Earthquake Center Publication 1792*, 97p, *http://pubs.usgs.gov/of/2013/1165/*

Gao, S. S., P. G. Silver, A. T. Linde, and I. S. Sacks (2000), Annual modulation of triggered seismicity following the 1992 Landers earthquake in California, *Nature*, *406*, 500-504.

Hainzl, S., Y. Ben-Zion, C. Cattania, and J. Wassermann (2013), Testing atmospheric and tidal earthquake triggering at Mt. Hochstaufen, Germany, *Journal of Geophysical Research: Solid Earth*, *118*(10), 5442-5452, doi:10.1002/jgrb.50387.

Hardebeck, J. L., and A. J. Michael (2006), Damped Regional-Scale Stress Inversions: Methodology and Examples for Southern California and the Coalinga Aftershock Sequence, *J .Geophys. Res.*, *111*(B11310), doi:10.1029/2005JB004144.

Heki, K. (2003), Snow load and seasonal variation of earthquake occurrence in Japan, *Earth and Planetary Science Letters*, *207*(1), 159-164, doi:10.1016/S0012-821X(02)01148-2.

Holzer, T. L. (1979), Elastic expansion of the lithosphere caused by groundwater depletion, *J .Geophys. Res.*, *84*, 4689–4698.

Johnson, C. W., Y. N. Fu, and R. Burgmann (2017), Seasonal water storage, stress modulation, and California seismicity, *Science*, *356*(6343), 1161-1164, doi:10.1126/science.aak9547.

Kilb, D., and J. L. Hardebeck (2006), Fault Parameter Constraints Using Relocated Earthquakes: A Validation of First-Motion Focal-Mechanism Data, *Bulletin of the Seismological Society of America*, *96*(3), 1140-1158, doi:10.1785/0120040239.

Namias, J. (1989), Summer earthquakes in southern California related to pressure patterns at sea level and aloft, *J. Geophys. Res.*, *94*(B12), 17671-17679, doi:10.1029/89JB01463.

Parsons, T. (2006), Tectonic stressing in California modeled from GPS observations, *J. Geophys. Res.*, *111*(B03407), doi:10.1029/2005JB003946.

Pollitz, F. F. (1996), Coseismic deformation from earthquake faulting on a spherical earth, *Geophysical Journal International*, *125*, 1-14.

Pollitz, F. F. (1997), Gravitational viscoelastic postseismic relaxation on a layered spherical Earth, *Journal of Geophysical Research*, *102*(B8), 17921, doi:10.1029/97jb01277.

Pollitz, F. F., A. G. Wech, H. Kao, and R. Bürgmann (2013), Annual modulation of non-volcanic tremor in northern Cascadia, *J .Geophys. Res.*, *118*, doi:10.1002/jgrb.50181.

Reasenberg, P. (1985), Second-order moment of central California seismicity, 1969-82, *J .Geophys. Res.*, *90*, 5479-5495.

Reasenberg, P. A., and D. H. Oppenheimer (1985), FPFIT, FPPLOT, and FPPAGE: FORTRAN computer programs for calculating and displaying earthquake fault-plane solutions, *U.S. Geol. Surv. Open File Rept*, 85-739.

Shen, Z. K., Q. Wang, R. Bürgmann, Y. Wan, and J. Ning (2005), Pole tide modulation of tremor and slow slip events at circum-pacific subduction zones, *Bull. Seism. Soc. Am.*, *95*(5), 2009-2015, doi:10.1785/0120050020.

Smith, B. R., and D. T. Sandwell (2006), A model of the earthquake cycle along the San Andreas Fault System for the past 1000 years, *J. Geophys. Res.*, *111*(B01405), doi:10.1029/2005JB003703.

Thomas, A. M., R. Bürgmann, D. R. Shelly, N. M. Beeler, and M. L. Rudolph (2012), Tidal triggering of low frequency earthquakes near Parkfield, CA: Implications for fault mechanics within the brittle-ductile transition, *J .Geophys. Res.*, *117*(B05301), doi:10.1029/2011JB009036.

van Stiphout, T., J. Zhuang, and D. Marsan (2012), Seismicity declustering, *Community Online Resource for Statistical Seismicity Analysis*, *Available at http://www.corssa.org/*, doi:10.5078/corssa-52382934.

Yang, W., and E. Hauksson (2013), The tectonic crustal stress field and style of faulting along the Pacific North America Plate boundary in Southern California, *Geophysical Journal International*, *194*(1), 100-117, doi:10.1093/gji/ggt113.

Zaliapin, I., and Y. Ben-Zion (2013), Spatio-temporal evolution of seismic clusters in southern and central California, *SCEC Annual Meeting Poster presentation*.

Zhuang, J., Y. Ogata, and D. Vere-Jones (2002), Stochastic declustering of space-time earthquake occurrences, *J. Am. Stat. Assoc.*, *97*, 369-382.